Research Square

Preprints are preliminary reports that have not undergone peer review. They should not be considered conclusive, used to inform clinical practice, or referenced by the media as validated information.

Evaluation of OAR sparing and plan robustness of beam-specific PTV in lung cancer IMRT treatment

Yu Chang
Huazhong University of Science and Technology
Feng Xiao
Wuhan University
Hong Quan
Wuhan Univeristy
Zhiyong Yang (284592664@qq.com)
Huazhong University of Science and Technology https://orcid.org/0000-0002-2806-1214

Research

Keywords: OAR sparing; plan robustness; van Herk's margin concept; beam specific PTV

Posted Date: July 17th, 2020

DOI: https://doi.org/10.21203/rs.3.rs-42810/v1

License: This work is licensed under a Creative Commons Attribution 4.0 International License. Read Full License

Version of Record: A version of this preprint was published on October 17th, 2020. See the published version at https://doi.org/10.1186/s13014-020-01686-1.

Loading [MathJax]/jax/output/CommonHTML/fonts/TeX/fontdata.js

Abstract

Purpose: Margins are employed in radiotherapy treatment planning to mitigate the dosimetric effects of geometric uncertainties for the clinical target volume (CTV). We propose a margin concept that takes the beam direction into consideration, generating a beam-specific PTV (BSPTV) on a beam entrance view. The total merged BSPTV was considered as target using for optimization. We investigated the impact of this novel approach when applied to lung IMRT treatments, and compared the treatment plans generated using BSPTV with conventional PTV.

Methods and Materials: We margin the BSPTV by expanding the CTV perpendicularly to the incident beam direction using the 2D version of van Herk's margin concept. The BSPTV and conventional PTV margin were first analyzed in digital phantom simulation. Then, fifteen lung cancer patients were used in this planning study. First, all patient targets were performed with the CTV projection area analysis to select the suitable beam angles. Then, BSPTV were margined according to the selected beam angles. IMRT plans were optimizted with the conventional PTV and BSPTV as the target volumes, respectively. The dosimetry metrics were calculated and evaluated between these two plans. The plan robustness of both plans for setup uncertainties was evaluated with worst-case analysis.

Results: Both conventional PTV and BSPTV plans satisfied the CTV coverage. The BSPTV plans improved the sparing of high doses to target-surrounding lung tissues much better than the conventional PTV plans. Both D_{mean} of Ring PTV and Ring BSPTV were significantly lower in BSPTV plans (38.89Gy and 39.43Gy) than that in the conventional PTV plans (40.27Gy and 40.68Gy). The V20, V5 and mean lung dose of the affected lung were significant lower in BSPTV plans (16.20%, 28.75% and 8.93Gy) than that in the conventional PTV plans (16.69%, 29.22% and 9.18Gy). About 80% of target coverage in all uncertainty scenarios could be achieved for both conventional PTV and BSPTV plans.

Conclusions: The results suggested that the plan robustness can be guaranteed in both the BSPTV and conventional PTV plans. However, the BSPTV plans can spare the normal tissues such as lungs significant better than the conventional PTV plans.

Introduction

The intensity-modulated radiotherapy (IMRT) can deliver conformal dose distributions to the tumors. However, the inter-fractional uncertainties during the treatment result in deviations between the planned and the actual dose distributions [1–3]. These uncertainties can result in underdosing of the clinical target volume (CTV), or overdosing of organs at risk (OARs) [1].

Current clinical practice account for the uncertainties is using a safety margin which is defined as planning target volume (PTV) [4–6]. To achieve a higher probability of the CTV coverage under uncertainties, a larger margin for PTV is needed. However, these can lead to more dose being delivered to the surrounding normal tissues [7]. In the van Herk's PTV recipe, the uncertainties are separated into two types: the systematic and random uncertainties [4]. Systematic uncertainties, affect all treatment fractions in the same way, but vary stochastically across the patient population. They can be modeled as displacements of the CTV relative to the blurred dose distribution. Random uncertainties vary from treatment to treatment, and can be modeled as blurring of the cumulative dose distribution.

The geometric uncertainties included both the systematic and random uncertainties might not simply blur the cumulative dose distribution isotropically. In reality, photon beam radiation deposits exponentially attenuation dose with depth, and whilst the lateral fall-off is much sharper [1, 6]. In other words, small displacements in beam direction result in small deviations from the planned dose, whereas displacements perpendicular to beam direction can result in severe underdosing due to the target moving out of the beam penumbra [4]. It is therefore physically impossible to generate a dose distribution with negligible dose outside the PTV in photon radiation due to the low dose bath in the beam direction.

The per-beam margin concept was first proposed by Peter Park *et al.* in the proton radiation [8]. They first used this beam specific PTV concept to account for the setup and range uncertainties in the prostate and thoracic sites of the proton

Loading [MathJax]/jax/output/CommonHTML/fonts/TeX/fontdata.js

radiotherapy. Based on their study, we modified the van Herk's margin method, generating margins varies with beams' incident directions, only accounting for uncertainties perpendicular to beam incident directions.

Tsang *et al.* proposed modifications to the van Herk's margin concept by considering margins on the perpendicular direction of each beam in the prostate cancer radiotherapy [9, 10]. Ph Kamerling *et al.* also used their adapted beam dependent margin concept which combines the beam dependent margin and probabilistic planning optimization together to optimization the trade-off between the target coverage and the surrounding rectum and bladder sparing [11]. Their results showed that better OAR dose sparing using the adapted beam dependent margin could be achieved comparing to the conventional margin. However, the plan robustness between the conventional PTV optimization plan and their beam dependent PTV optimization plan wasn't compared.

The lung cancer radiation treatment is subject to the respiratory and setup uncertainties. The therapeutic ratio in lung cancer is essential to ensure adequate coverage of the moving target volume while sparing the surrounding normal tissues. In this study, we focused on generating margins that are dependent on the beams' incident directions, and merge them as a beam-specific PTV (BSPTV) in the lung cancer radiotherapy. Then we compared the dose distributions between the conventional PTV and BSPTV optimized IMRT plans. We also evaluated the plan robustness for the setup uncertainties between these two optimization strategy plans.

Materials And Methods

Patient cohort

Fifteen lung cancer patients treated with IMRT between September 2018 and December 2018 were selected for this retrospective study. All patients in this study were enrolled in an institutional review board-approved retrospective data collection protocol. Each patient had completed IMRT or SBRT treatments.

Patients were acquired 4DCT with the real-time position management system (RMP, Varian Medical Systems, Palo Alto, CA, USA). The gross tumor volume (GTV) was contoured on the average-weighted CT images. The GTV to clinical target volume (CTV) margin for inclusion of microscopic extension of the tumor was 2 mm. To simplify our analysis, only tumors in one side of lungs were selected. And all organs at risk (OARs), such as lungs and spinal cord were contoured on average-weighted CT images. The average-weighted CT images were used for plan optimization and dose calculation.

Beam-specific PTV concept

To generate the beam-specific PTV (BSPTV) for photon radiotherapy, we expanded the CTV perpendicularly to each incident beam direction using the 2D version of van Herk's margin concept. We chose not to add margin the CTV in the incident beam direction, since the percentage depth dose reduction in the incident beam direction is very small. We obtained the final BSPTV by merging each beam expansions together. Figure 1 shows the situations that we ignored the longitudinal (parallel to beam direction) margins and retained the transverse (perpendicular to beam direction) margins. Figure 2 shows the geometric differences between the original PTV and the BSPTV for the same CTV in the isocenter axial slice.

The inter-fractional uncertainties considered in this study are defined in the patient's left-right, anterior-posterior and superior-inferior directions, and are assumed to be normally distributed with no correlations between them. The collapse of the 3D Gaussian distribution, in beam direction, into a 2D Gaussian distribution has been defined with the van Herk's margin concept [4].

$$M = \alpha\Sigma + \beta\sqrt{\sigma^2 + \sigma_p^2} - \beta\sigma_p$$

Variables Σ, σ and σ_p are two-dimensional column vectors for the directions perpendicular to the incident beam angle, representing the systematic uncertainties, random uncertainties and the beam penumbra, defined as the distance between the 20% and 80% isodose levels, respectively. The beam penumbras (σ_p) was described by a Gaussian with SD = 3.2 mm in this

Loading [MathJax]/jax/output/CommonHTML/fonts/TeX/fontdata.js ded probability of target dose coverage are calculated by solving the closed-formed dose population histogram, following the integral formula in appendix 2 of the previous research [4]. Our method to calculate the 2D margin from the direction perpendicular to each beam is implemented as a standalone MATLAB (MathWorks, Natick, MA) program. In our programmed 2D margin script, to ensure that 90% of the patients receive at least 95% of the prescribed dose across the whole of the target, the corresponding coefficients are $\alpha = 2.15$ and $\beta = 1.64$. And we set the systematic uncertainties $\Sigma = 2$ mm, random uncertainties $\sigma = 2$ mm according to the previous research and our clinical results [4, 12], the Margin (M) $\approx$ 4.4 mm. The automatic generated 2D margins of each beam were imported into Eclipse TPS (Varian Medical Systems) and merged as the BSPTV for subsequent optimization. The conventional PTV is margined by the 3D van Herk's margin concept, with the same systematic and random uncertainties as the BSPTV, the systematic uncertainties $\Sigma =$ 2 mm, random uncertainties $\sigma = 2$ mm, $\alpha = 2.5$ and $\beta = 1.64$, the M $\approx$ 5 mm.

Phantom Simulation

A digital water phantom simulation is used to evaluate the conformity of the dose distribution to the OAR sparing of these two margin concepts. In this simulation model, the tumor consisted of a spherical CTV of 4 cm diameter, which corresponds roughly to the average CTV sizes with our patient data. Two types of 50 Gy/25F treatment plans were designed for both general PTV and BSPTV and the generated dose distributions were such that 98% of the PTV received 100% of the prescribed dose. The conventional PTV margin (M $\approx$ 5 mm) was applied around the GTV for the plans with conventional PTV as target volume. The BSPTV margin (M $\approx$ 4.4 mm, in 0°, 30°, 60° and 90° in directions) was applied around the GTV for the plans with BSPTV as target volume. First type were two clinical IMRT plans using 4 coplanar beams with 0°, 30°, 60° and 90° with the conventional PTV and BSPTV as the target volume, respectively. The plan conformity index (CI, $CI = 100\% \cdot [TV_{PI}]^2/[PI_{100} \cdot TV]$) were optimized to keep the CI in both general PTV and BSPTV plans above 80%. TV is the target volume, TV_{PI} is the volume of the target covered by the prescribed isodose, and PI_{100} is the volume receiving 100% of the prescribed isodose; conformity is better as the index approaches 100%. Second type were hypothetical plans with an ideal dose distribution (such as a VMAT plan with spherically symmetric dose that falls off in all directions), resulting in CI above 90%.

CTV projection area analysis

We analyzed the mathematical relationship between the margin volume and the projection area of the target. The calculation and analysis details are showed in appendix 1. Based on a patient's CT data set, we calculated the CTV projection area in a beam direction from 0° to 359°. Since the BSPTV of a beam is a 2D margin of CTV in the beam direction, the projection area of CTV in the beam direction is an index to evaluate the volume of 2D expansion of the CTV. The projection area of CTV was calculated for a full circle of beam angles (0°-359°) at increments of 1° to yield a patient-specific CTV projection area curve as a function of beam angle. As an example, Fig. 3(a) shows one patient's CTV projection area with respect to the beam angle.

IMRT planning

IMRT plans were prescribed to 60 Gy in 30 fractions with 6 MV X-ray. First, we selected 4 to 5 beam angles according to the CTV projection area curve to make sure the 2D margins of each beam could be the maximum. We also set most beams incident in the AP directions, to avoid the beam penetrating both lungs. Second, we margined the conventional PTV and BSPTV as the description in Beam-specific PTV concept Section for comparison. We designed 2 plan optimization strategies to compare the dose distribution differences between the conventional PTV and BSPTV. The optimization objective for all plans was to achieve 100% of the prescribed dose to the target volume first and then to minimize the dose to OARs. We first optimized all patients' plans on the target volume of the conventional PTV. Then we kept all optimization objective parameters unchanged; copied a new plan and only changed the target volume to BSPTV, then re-optimize this BSPTV plan. After both plan optimizations completed, all plans were normalized to facilitate dose comparisons. The normalization point was the target $D_{98\%}$ of 60 Gy, where $D_{x\%}$ was defined as the lowest dose covering x% of the volume. To exclude the influence of the conformity of the dose distribution to the plan evaluation, the plans with CI below 80% were re-optimized until above 80%.

Plan evaluation

Loading [MathJax]/jax/output/CommonHTML/fonts/TeX/fontdata.js

To quantify the differences between the conventional PTV and BSPTV plans, dose-volume histograms were used to assess the dose coverage and conformity of targets and the protection of OARs. The target evaluation parameters were D98% (target coverage), D2%, conformity index (CI), and homogeneity index (HI) [13]. The HI, defined as 100% × $(D_{2\%} - D_{98\%})/D_{50\%}$, was used to evaluate dose homogeneity within each target volume; plans that are more homogenous have HI values closer to 0% [13]. V5, V20 and mean doses to both lungs were compared. For the spinal cord, the $D_{1\%}$ was compared. In order to evaluation the adjunction normal tissue of CTV, a 2 cm ring of CTV was margined as CTV margin. The Ring PTV or Ring BSPTV was created by CTV margin subtract the conventional PTV or BSPTV. The volume and mean doses of Ring PTV and Ring BSPTV were compared.

Robust analysis

The inter-fractional uncertainties occurred between treatment fractions, such as set-up uncertainties and anatomical variations over the course of radiation therapy. In this study, we evaluated the set-up uncertainties using the uncertainty dose evaluation of Eclipse treatment planning system (Varian Medical Systems, Palo Alto, CA), assuming the inter-fractional setup uncertainties of ± 5 mm in AP, LR and SI directions, total 6 scenarios. Since the van Herk margin recipe is designed for 90% of coverage of the patients with a minimal dose of 95% to 100% of the target volume. The ratio of scenarios satisfied the clinical specification that the 100% of CTV being above the 95% prescription dose was evaluated.

Statistics analysis

SPSS 24.0 software (IBM, Armonk, NY) was used for statistical analyses of all dosimetric metrices. We conducted a paired, two-tailed Wilcoxon signed-rank test to compare the dose distributions between the conventional PTV and BSPTV plans. *P* values of less than 0.05 were considered statistically significant.

Results

Phantom Simulation

Table 1 shows the phantom simulation results of the 4-field IMRT plans and the hypothetical plans with ideal dose distribution. For the plans with PTV set as target volume, the CI of 4-field IMRT plans is 85.18% and the CI of the hypothetical plans with ideal dose distribution is 92.80%. The mean value of Ring PTV is 53.08 Gy in 4-field IMRT plans and 53.34 in the hypothetical plans with ideal dose distribution. For the plans with BSPTV set as target volume, the CI of 4-field IMRT plans is 83.25% and the CI of the hypothetical plans with ideal dose distribution is 91.92%. The mean value of Ring PTV is 52.89 Gy in 4-field IMRT plans and 52.97 in the hypothetical plans with ideal dose distribution. Both 4-field IMRT plans and the hypothetical plans with ideal dose distribution are 100% satisfied the clinical specification of plan robustness, as shown in table 2.

Table 1. Summary of dose to targets and OARs in water phantom simulation

Loading [MathJax]/jax/output/CommonHTML/fonts/TeX/fontdata.js

Parameter	conventional PTV 4-field IMRT plan	BSPTV 4-field IMRT plan	conventional PTV ideal dose distribution plan	BSPTV ideal dose distribution plan
CTV, $D_{98\%}$	62.5	62.5	61.5	61.0
Conventional PTV, Volume (cm^3)	65.9	65.9	65.9	65.9
Conventional PTV, $D_{98\%}$ (Gy)	60	59.9	60	59.5
Conventional PTV, $D_{2\%}$ (Gy)	64.5	64.6	63.3	63.4
Conventional PTV, CI (%)	85.18	85.09	92.80	91.07
Conventional PTV, HI (%)	3.51	3.59	3.39	3.41
BSPTV, Volume (cm^3)	62.5	62.5	62.5	62.5
BSPTV, $D_{98\%}$ (Gy)	60.1	60	60.2	60
BSPTV, $D_{2\%}$ (Gy)	64.5	64.6	63.3	63.4
BSPTV, CI	82.44	83.25	90.73	91.92
BSPTV,HI	3.50	3.57	3.38	3.39
Ring PTV, D_{mean} (Gy)	53.08	52.42	53.34	52.59
Ring BSPTV, D_{mean} (Gy)	53.53	52.89	53.73	52.97
Ring PTV, Volume (cm^3)	61.2	61.2	61.2	61.2
Ring BSPTV, Volume (cm^3)	64.6	64.6	64.6	64.6

Abbreviations: HI = homogeneity index; CI = conformity index.

Table 2. The ratios of scenarios satisfied the clinical specifications that the 100% target volume being above the 100% or 95% prescription dose in water phantom simulation

Plan name	Conventional PTV plan (%)		BSPTV plan (%)	
	100% prescription dose	95% prescription dose	100% prescription dose	95% prescription dose
4-field IMRT plan	67	100	67	100
ideal dose distribution plan	67	100	67	100

CTV projection area analysis

The shapes of CTV projection area curve for different patients were found to be varied. In our mathematical and geometrical analysis (Appendix 1), the results suggested that the smallest volume of BSPTV is obtained with the beam irradiated perpendicular to the maximum average length of the target in the XOY plane. Table 3 lists the beam angles corresponding to the first and second maximum values of CTV projection area for each patient.

Volume difference between the conventional PTV and BSPTV

Beams were selected according to the CTV projection area curve. A larger CTV projection area indicates a smaller 2D expansion of the CTV and more sparing of the adjacent OARs. The beam angles of an example case are shown in Fig. 3(b). Table 3 lists the volume of the conventional PTVs and BSPTVs for all patients. The mean (SD) volume reduction of the BSPTV comparing to the conventional PTV is -10.27% (7.11 %) for all patients.

Table 3. Volumes for conventional PTVs and the union of BSPTVs for all patients, and the beam angles corresponding to the extreme values of ITV projection area and the plan selected beam angles

Patient number	CTV Volume (cm^3)	Conventional PTV Volume (cm^3)	BSPTV Volume (cm^3)	Volume Difference (%)	Beam angles for maximum, 2nd maximum ITV projection area	Selected beam angles
1	36.9	83.9	76	-10.39	204, 180	90, 150, 180, 230
2	11.5	29.2	27.9	-4.66	175, 210	21, 150, 180, 210, 335
3	6.7	22.9	18.8	-21.81	300, 320	0, 30, 170, 300
4	87.7	164.5	153.9	-6.89	102, 90	0, 30, 160, 190, 220
5	12.6	35	30.3	-15.51	90, 315	0, 90, 175, 315
6	3.1	12.9	11.3	-14.16	195, 180	70, 130, 180, 210
7	270.9	466.2	443.6	-5.10	0, 220	0, 30, 160, 220, 290
8	10.2	27.6	25.6	-7.81	106, 320	10, 40, 180, 330
9	1.5	9	7	-28.57	160, 125	40, 130, 180, 210
10	57.6	155.4	146.3	-6.22	45, 90	40, 95, 175, 225
11	12.33	32.88	31.32	-4.98	0,210	0,130,170,210
12	8.91	31.09	28.080	-10.72	130,145	15,150,180,210,240
13	72.69	102.8	99.8	-3.01	320,50	320,40,0,170
14	9.43	25.97	24.6	-5.57	270,240	240,210,180,150,15
[illegible]	[illegible]	[illegible]	[illegible]	[illegible].72	250,180	210,180,150,120,345

Loading [MathJax]/jax/output/CommonHTML/fonts/TeX/fontdata.js

Dose difference between the conventional PTV optimization plan and BSPTV optimization plan

Table 4 shows the conventional PTV and BSPTV $D_{98\%}$, $D_{2\%}$, CI, and HI for the two plans. For all patients, the $D_{2\%}$ of conventional PTV and BSPTV did not significantly differ between the conventional PTV and BSPTV plans. The CI of Conventional PTV in the conventional PTV optimization plan and the CI of BSPTV in the BSPTV optimization plan were no significantly different (p = 0.281). The CI of BSPTV was higher in the BSPTV optimization plan than that in the conventional PTV plan (p = 0.003). The $D_{98\%}$ of BSPTV was higher than that of the conventional PTV in both conventional PTV plans (p = 0.003) and BSPTV plans (p = 0.001).

The volume of Ring PTV was smaller than the volume of Ring BSPTV (p = 0.001). The BSPTV plans had significantly lower mean dose for Ring PTV and Ring BSPTV than did the conventional PTV plan (p = 0.001 and p = 0.001). Compared with the conventional PTV plans, the BSPTV plans showed a decrease in the V5 and mean dose of the affected lung (p = 0.013, 0.005), contralateral lung (p = 0.028, 0.012) and total lungs (p = 0.015, 0.003) and a decrease in the V20 of the affected lung (p = 0.005) and total lungs (p = 0.008).

Table 4. Summary of dose to targets and OARs for all patients, shown as mean (standard deviation)

Parameter	conventional PTV optimization plan	BSPTV optimization plan	P^a
CTV, $D_{98\%}$ (Gy)	61.68(0.99)	61.40(1.15)	0.280
Conventional PTV, $D_{98\%}$ (Gy)	60(0)	58.84(1.01)	0.001^*
Conventional PTV, $D_{2\%}$ (Gy)	63.38(1.35)	63.36(1.53)	0.649
Conventional PTV, CI	0.85(0.05)	0.86(0.05)	0.233
Conventional PTV, HI	0.05(0.02)	0.07(0.03)	0.002^*
BSPTV, $D_{98\%}$ (Gy)	60.53(0.5)	60(0)	0.003^*,0.003^{*c},0.001^{*d}
BSPTV, $D_{2\%}$ (Gy)	63.48(1.41)	63.36(1.51)	0.975
BSPTV, CI	0.79(0.07)	0.84(0.05)	0.003^*,0.281^e
BSPTV,HI	0.05(0.02)	0.05(0.02)	0.100
Ring PTV, D_{mean} (Gy)	40.27(6.83)	38.89(7.13)	0.001^*
Ring BSPTV, D_{mean} (Gy)	40.68(6.72)	39.43(7.08)	0.001^*
Ring PTV, Volume (cm^3)	195.61(203.99)		0.001^{*b}
Ring BSPTV, Volume (cm^3)	201.21(210.89)		
Affected lung, V20	16.69(11.32)	16.20(10.85)	0.005^*
Contralateral lung, V20	0.36(0.01)	0.36(0.01)	1.000
Total Lungs, V20	7.25(6.40)	7.02(6.00)	0.008^*
Affected lung, V5	29.22(14.87)	28.75(14.43)	0.013^*
Contralateral lung, V5	6.91(11.71)	6.71(11.56)	0.028^*
Total Lungs, V5	16.26(12.72)	15.92(12.37)	0.015^*
Affected lung, D_{mean} (Gy)	9.18(5.51)	8.93(5.28)	0.005^*
Contralateral lung, D_{mean} (Gy)	0.97(1.43)	0.95(1.42)	0.012^*
Total Lungs, D_{mean} (Gy)	4.79(3.33)	4.67(3.18)	0.003^*
Spinal cord, $D_{1\%}$ (Gy)	16.14(16.50)	15.72(15.89)	0.009^*

Abbreviations: HI = homogeneity index; CI = conformity index.

[a]Comparison of conventional PTV optimization plan with BSPTV optimization plan

[b]Comparison of Volumes of Ring PTV and Ring BSPTV

[c]Comparison of $D_{98\%}$ of Conventional PTV and BSPTV in the same conventional PTV optimization plan

[d]Comparison of $D_{98\%}$ of Conventional PTV and BSPTV in the same BSPTV optimization plan

[e]Comparison of CI of Conventional PTV in the conventional PTV optimization plan and CI of BSPTV in the BSPTV optimization plan

$^*P < 0.05$

Robust analysis

Table 5 shows the results of robust analysis for both conventional PTV plans and BSPTV plans. The ratios of scenarios satisfied that the 100% of CTV volume could still be above the 100% or 95% (clinical specification) of the prescription dose were calculated for both plans. The results showed that the ratios of scenarios satisfied the clinical specifications were not significantly different between the conventional PTV and BSPTV plans (mean value: 0.966 vs. 0.953, p = 0.317). About 80% of target coverage could still be achieved in all uncertainty scenarios for both conventional PTV and BSPTV plans.

Loading [MathJax]/jax/output/CommonHTML/fonts/TeX/fontdata.js

Table 5. The ratios of scenarios satisfied the clinical specifications that the 100% target volume being above the 100% or 95% prescription dose for all patients

Patient number	Conventional PTV plan (%)		BSPTV plan (%)	
	100% prescription dose	95% prescription dose	100% prescription dose	95% prescription dose
1	50	100	50	100
2	50	100	50	100
3	100	100	50	100
4	100	100	100	100
5	67	83	50	83
6	50	100	50	100
7	100	100	100	100
8	67	100	67	100
9	83	100	67	83
10	100	100	100	100
11	100	100	83	100
12	67	100	50	100
13	17	67	17	67
14	83	100	83	100
15	100	100	100	100

Discussion

Comparing to the proton radiotherapy, the photon radiotherapy inability to physically produce perfectly conforming dose distributions, as there will also be a presence of entrance and exit doses due to how photons interact with matter. However, we took advantage of the exponential relationship between the absorbed dose and radiological depth. Since the small movements in the beam direction result in negligible dose deviation, we designed the BSPTV concept to sparing more normal tissues in the beam direction. Because of the different shapes of the target in different beam entrance directions, it is important to choose the suitable incidence angle of the beam according to the projection area values. But it still needs to consider the surrounding OARs when choosing the incidence angle of the beam. Moreover, the distance of the target to the field isocenter is related to the utilization efficiency of the radiation, the choosing of the incident angle of the beam is a trade-off between the different factors.

According to the previous research, the suboptimal dose conformation could lead to a tighter margin for the target, because of the prescription dose escaping outside to the target. [14]. In our phantom simulation, a better conformity target dose distribution is achieved in the hypothetical plans group (> 90%)than in the 4-field IMRT plans group (> 80%). But the plan robustness are not different between these two types of plans. These results suggest that the conformity of dose distribution would not have much impact on the plan robustness when high target conformity (> 80%) has been achieved. Since now high target conformity (> 80%) could easily be achieved in IMRT plans, the plan robustness would not be subject to the conformity of the dose distribution.

We chose the CTV projection area analysis to find the suitable beam angles to obtain the smaller BSPTV volume and sparing more lung tissues. The mathematical and geometrical analysis suggested that the beam irradiated perpendicular to the maximum average length of the target in the XOY plane which means the target projection area is the maximum in this beam entrance view will obtain the minimum BSPTV volume. Especially for those targets with irregular shape, such as the example case in Fig. 3, the CTV projection area differences between the maximum value and minimum value could be 25%, as shown in Fig. 3(a). The CTV projection area curve is symmetric for beam angles with 180° intervals. We could choose the suitable beam angles according to CTV projection area curve with a direction close to the tumor.

Loading [MathJax]/jax/output/CommonHTML/fonts/TeX/fontdata.js

With the beam angles increasing from 3 beams to 5 beams, the volume differences between the conventional PTV and BSPTV became gradually smaller. The BSPTV concept is not suitable for the large number of beams treatment, such as SBRT, since the BSPTV volume might be the same with the conventional PTV.

Nadya Shusharina *et al.* proposed the probabilistic clinical target distribution concepts implemented into the probabilistic optimization process in the head and neck cases [15]. It allows physicists and physicians find the most suitable trade-off between the target coverage and sparing of surrounding normal tissues at the treatment planning stage, without having to modify or redraw a CTV. Marnix G Witte *et al.* also tested the probabilistic planning margin volume concepts in the simulated phantom [16]. Watkins *et al.* defined the definite target volume to deliver extremely high doses to sub-volumes of PTVs in multiple treatment sites [17]. These three studies both focused on the influence of the probabilistic dose distribution to the target coverage and sparing of surrounding normal tissues and is another strategy comparing to the BSPTV methods. Since the BSPTV strategy could be applied without modification of optimization engine of the commercial treatment planning system, it is much easier and more straightforward.

A considerable amount of work remains to continue to improve BSPTV optimization. Both van Herk's margin concept and our beam specific margin concept share the assumptions: the treatment uncertainties follow a Gaussian distribution, and only rigid translations of the target were accounted for [4]. We will focus on the effects of the rotation and deformation uncertainties of the targets. And we will continue study the BSPTV of two or more targets in one patient, such as primary sites and mediastinal lymph nodes for lung cancer cases.

Conclusion

The lung tumors are surrounding by the normal tissues and OARs, and the low dose to the normal tissues needs to be carefully. Hence, the IMRT plans treated the lung tumors are usually 4–5 beams to control the low dose area, these plan strategy is very suitable for using BSPTV.

Abbreviations

CTV: Clinical target volume; PTV: Planning target volume; BSPTV: Beam-specific PTV; IMRT: Intensity modulated radiation therapy; OAR: Organ at risk; DVH: Dose volume histogram; SBRT: Stereotactic body radiation therapy; GTV: gross tumor volume; SD: standard deviation

Declarations

Acknowledgments

This work was supported by National Natural Science Foundation of China (Grant No.81803047) (ZY) and the Fundamental Research Funds for the Central Universities of China (Grant No. 2019kfyXKJC061) (ZY).

Ethics approval and consent to participate

All patients in this study were enrolled in an institutional review board of Tongji Medical College, Huazhong University of Science and Technology-approved retrospective data collection protocol.

Consent for publication

Not applicable.

Availability of data and materials

Please contact author for data requests.

Loading [MathJax]/jax/output/CommonHTML/fonts/TeX/fontdata.js

The authors declare that they have no competing interests.

Funding

1) National Natural Science Foundation of China (Grant No.81803047)

2) Fundamental Research Funds for the Central Universities of China (Grant No. 2019kfyXKJC061)

Authors' contributions

Dr. Zhiyong Yang and Dr. Feng Xiao developed the 2D version of van Herk's margin program and performed all the calculation. Dr. Yu Chang helped to collect data and participated in the research design. Dr. Yu Chang, Dr. Hong Quan and Dr. Zhiyong Yang drafted the manuscript. All authors read and approved the final manuscript.

References

1. Yoon M, Kim D, Shin DH, Park SY, Lee SB, Kim DY, et al. Inter- and Intrafractional Movement–Induced Dose Reduction of Prostate Target Volume in Proton Beam Treatment. International Journal of Radiation Oncology*Biology*Physics. 2008;71:1091–102.
2. Chang Y, Liu H-Y, Liang Z-W, Nie X, Yang J, Liu G, et al. Dosimetric Effect of Intrafraction Tumor Motion in Lung Stereotactic Body Radiotherapy Using CyberKnife Static Tracking System. Technol Cancer Res Treat. 2019;18:1533033819859448.
3. Yang Z, Chang Y, Brock KK, Cazoulat G, Koay EJ, Koong AC, et al. Effect of setup and inter-fraction anatomical changes on the accumulated dose in CT-guided breath-hold intensity modulated proton therapy of liver malignancies. Radiother Oncol. 2019;134:101–9.
4. van Herk M, Remeijer P, Rasch C, Lebesque JV. The probability of correct target dosage: dose-population histograms for deriving treatment margins in radiotherapy. International Journal of Radiation Oncology*Biology*Physics. 2000;47:1121–35.
5. van Herk M, Remeijer P, Lebesque JV. Inclusion of geometric uncertainties in treatment plan evaluation. International Journal of Radiation Oncology*Biology*Physics. 2002;52:1407–22.
6. McKenzie AL, Herk Mv, Mijnheer B. The width of margins in radiotherapy treatment plans. Phys Med Biol. 2000;45:3331–42.
7. Lin L, Kang M, Huang S, Mayer R, Thomas A, Solberg TD, et al. Beam Specific Planning Target Volumes Incorporating 4DCT for Pencil Beam Scanning Proton Therapy of Thoracic Tumors. Med Phys. 2015;42:3365-.
8. Park PC, Zhu XR, Lee AK, Sahoo N, Melancon AD, Zhang L, et al. A Beam-Specific Planning Target Volume (PTV) Design for Proton Therapy to Account for Setup and Range Uncertainties. International Journal of Radiation Oncology*Biology*Physics. 2012;82:e329-e36.
9. Tsang HS, Kamerling CP, Ziegenhein P, Nill S, Oelfke U. A novel probabilistic approach to generating PTV with partial voxel contributions. Phys Med Biol. 2017;62:4917–28.
10. Tsang HS, Kamerling CP, Ziegenhein P, Nill S, Oelfke U. Novel adaptive beam-dependent margins for additional OAR sparing. Phys Med Biol. 2018;63:215019.
11. Ph Kamerling C, Ziegenhein P, Sterzing F, Oelfke U. Interactive dose shaping part 2: proof of concept study for six prostate patients. Phys Med Biol. 2016;61:2471–84.
12. Yang Z-Y, Chang Y, Liu H-Y, Liu G, Li Q. Target margin design for real-time lung tumor tracking stereotactic body radiation therapy using CyberKnife Xsight Lung Tracking System. Sci Rep. 2017;7:10826.
13. Yang Z, Zhang X, Wang X, Zhu XR, Gunn B, Frank SJ, et al. Multiple-CT optimization: An adaptive optimization method to account for anatomical changes in intensity-modulated proton therapy for head and neck cancers. Radiother Oncol. 2020;142:124–32.

Loading [MathJax]/jax/output/CommonHTML/fonts/TeX/fontdata.js

14. Stroom J, Gilhuijs K, Vieira S, Chen W, Salguero J, Moser E, et al. Combined Recipe for Clinical Target Volume and Planning Target Volume Margins. International Journal of Radiation Oncology*Biology*Physics. 2014;88:708–14.
15. Shusharina N, Craft D, Chen Y-L, Shih H, Bortfeld T. The clinical target distribution: a probabilistic alternative to the clinical target volume. Phys Med Biol. 2018;63:155001.
16. Witte MG, Sonke J-J, Siebers J, Deasy JO, van Herk M. Beyond the margin recipe: the probability of correct target dosage and tumor control in the presence of a dose limiting structure. Physics in medicine biology. 2017;62:7874–88.
17. Watkins WT, Nourzadeh H, Siebers JV. Dose escalation in the definite target volume. Med Phys. 2020;in press.

Appendix 1

The relationship of the margin volume and the projection area of the target

The total projection areas (S_{YOZ}) of the target volume in a beam direction from 0° to 359° were calculated. In this research, CTV is the target. The margin volume of the convention PTV margin receipt will be:

$$V_{PTV}= \int_0^{x_0+2m}\int_0^{y_0+2m}\int_0^{z_0+2m}dxdydz$$

A1

where m is the length of the margin, V_{PTV} is the volume of PTV.

The margin volume of the BSPTV margin receipt will be:

$$V_{BSPTV}= \int_0^{x_0}\int_0^{y_0+2m}\int_0^{z_0+2m}dxdydz$$

A2

where m is the length of the margin, V_{BSPTV} is the volume of BSPTV.

The volume differences between the two margin receipts are as following:

$$\Delta V= V_{PTV}- V_{BSPTV}= \int_0^{x_0+2m}\int_0^{y_0+2m}\int_0^{z_0+2m}dxdydz- \int_0^{x_0}\int_0^{y_0+2m}\int_0^{z_0+2m}dxdydz= \int_0^{2m}\int_0^{y_0+2m}\int_0^{z_0+2m}dxdydz$$

A3

ΔV is the volume differences between the two margin receipts.

If we need to spare more normal tissues, the ΔV needs to be the maximum. Hence, $\int_0^{y_0+2m}\int_0^{z_0+2m}dydz$ needs to be the maximum. Since the $\int_0^{y_0+2m}\int_0^{z_0+2m}dydz$ is in direct proportion to S_{YOZ}, the beam angle for the maximum of S_{YOZ} might be chose as the best beam angle to sparing the surrounding normal tissues.

Without loss of generality, we took the target as an ellipsoid with the lengths of axis (a (X axis) > b (Y axis) > c (Z axis)) as shown in Fig. 4 for example. The margin volume of the ellipsoid using the convention PTV margin receipt will be:

$$V_{PTV-ellipsoid}= \int_0^{x_0+2m}\int_0^{y_0+2m}\int_0^{z_0+2m}dxdydz= \frac{4}{3}\pi(a+2m)\cdot(b+2m)\cdot(c+2m)$$

A4

where m is the length of the margin, $V_{PTV-ellipsoid}$ is the margin volume of the ellipsoid using the convention PTV margin receipt.

$$V_{BSPTV-ellipsoid}= \int_0^{x_0}\int_0^{y_0+2m}\int_0^{z_0+2m}dxdydz= \frac{4}{3}\pi(c+2m)\int_0^{x_0}\int_0^{y_0+2m}dxdy$$

Loading [MathJax]/jax/output/CommonHTML/fonts/TeX/fontdata.js

A5

where m is the length of the margin, $V_{BSPTV-ellipsoid}$ is the margin volume of the ellipsoid using the BSPTV margin receipt. The maximum of $V_{BSPTV-ellipsoid}$ is $\frac{4}{3}\pi a \cdot (b+2m) \cdot (c+2m)$ with the beam angle paraell to the X axis. The minimum of $V_{BSPTV-ellipsoid}$ is $\frac{4}{3}\pi(a+2m) \cdot b \cdot (c+2m)$ with the beam angle paraell to the Y axis.

The volume differences between the two margin receipts are as following:

$$\Delta V_{ellipsoid} = V_{PTV-\,ellipsoid} - V_{BSPTV-\,ellipsoid} = 2m \cdot \int_0^{y_0+2m}\int_0^{z_0+2m} dydz = 2m \cdot S_{YOZ(\,marg\ in)}$$

A6

$\Delta V_{ellipsoid}$ is the volume differences between the two margin receipts.

In order to obtain the maximum $\Delta V_{ellipsoid}$, the S_{YOZ} needs to be the maximum as following:

$$S_{YOZ(\,marg\ in)} \overset{\Delta max}{=} \pi(a+2m) \cdot (c+2m)$$

A7

$$\Delta V_{ellipsoid} = V_{ellipsoid} - V_{BSellipsoid} = 2m \cdot \int_0^{y_0+2m}\int_0^{z_0+2m} dydz = 2m \cdot S_{YOZ(\,marg\ in)} \overset{\Delta max}{=} \frac{8}{3} m\pi(a+2m) \cdot (c+2m)$$

A8

Where the beam angle for the maximum of S_{YOZ} is parallel to the Y axis and perpendicular to the X axis, the $\Delta V_{ellipsoid}$ is maximum and the $V_{BSellipsoid}$ is the smallest. As shown in Fig. 4(c), the beam angle for the maximum of S_{YOZ} is 90° in this ellipsoid case, and the beam angle for the mimmum of S_{YOZ} is 0° in this ellipsoid case.

Generalize to the general case, the value of S_{YOZ} is calculated as the product of the average length of target in the Z axis and the average length of target in the XOY plane. Since the beam is irradiated perpendicular to the Z axis, the average length of target in the Z axis is relatively a constant. Hence, the average length of target in the XOY plane will determine the value of S_{YOZ}. The smallest volume of BSPTV is obtained with the beam irradiated perpendicular to the maximum average length of the target in the XOY plane.

Figures

Loading [MathJax]/jax/output/CommonHTML/fonts/TeX/fontdata.js

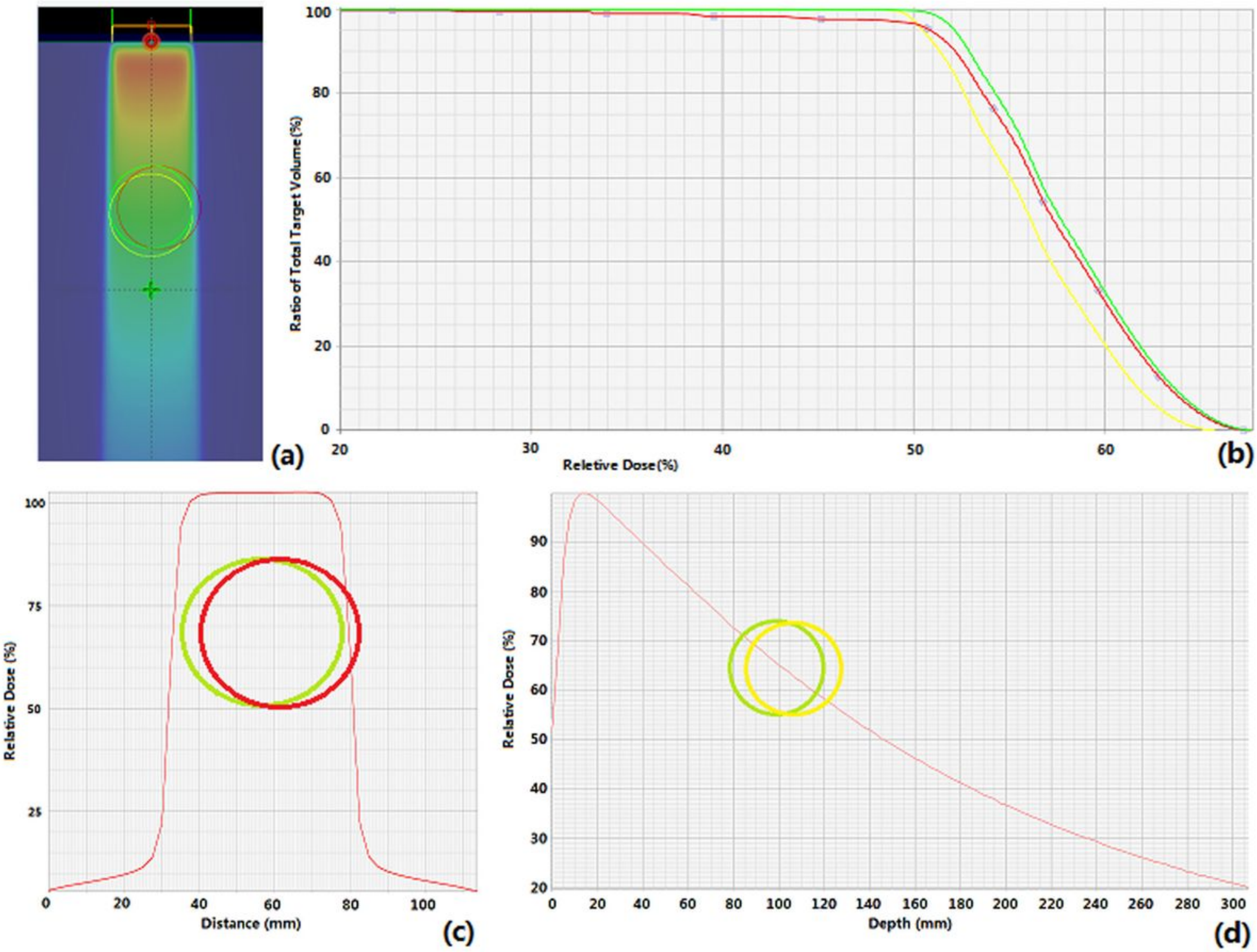

Figure 1

The original target position is indicated by the green circle, (a) Target movements for photon irradiation in beam direction (yellow circle) and perpendicular to beam direction (red circle); (b) The DVH of static target (green line) and targets moving in beam direction (yellow line) and perpendicular to beam direction (red line); (c) Dose profile between the original target (green circle) and the moved target for photon beam perpendicular to beam direction (red circle); (d) Percentage depth dose between the original target (green circle) and the moved target for photon beam in the beam direction (yellow line).

Loading [MathJax]/jax/output/CommonHTML/fonts/TeX/fontdata.js

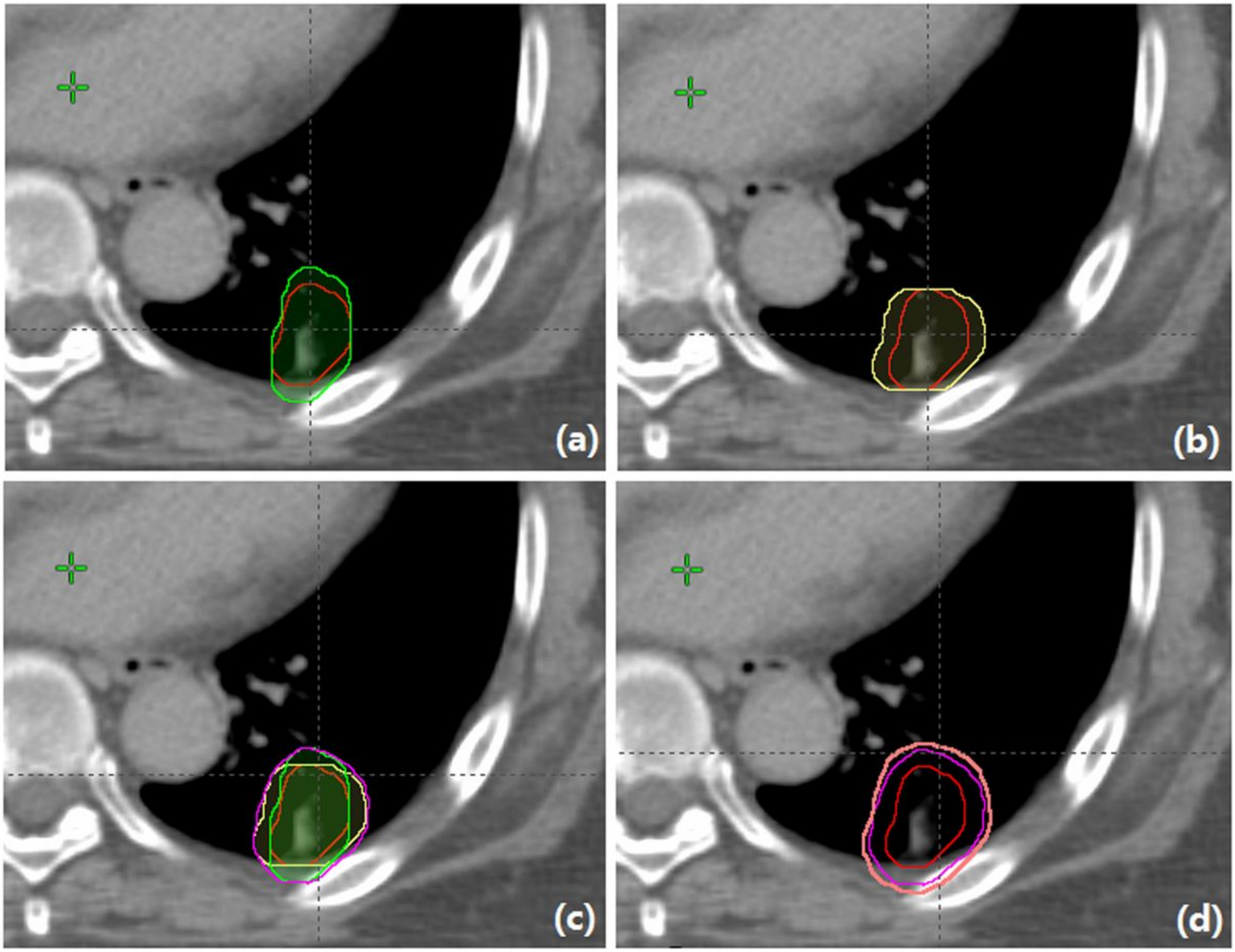

Figure 2

e isocenter axial slice of the CTV (red line) expansion generated using 2D VHMR for 90° beam (green line) in panel (a) and 180° beam (yellow line) in panel (b); Panel (c) shows the isocenter axial slices of the union BSPTV for all beams (pink line); Panel (d) shows the isocenter axial slices of the union BSPTV (pink line) and conventional PTV (light brown line).The example case's CTV projection area with respect to the beam angle is shown in panel (a). The selected beam angles (0°, 30°, 160°, 220°, and 290°) are indicated as green circles. The first and second maximum projection beam angles are indicated as red triangles; The axial slice view of the example case's beams are shown in panel (b).

Loading [MathJax]/jax/output/CommonHTML/fonts/TeX/fontdata.js

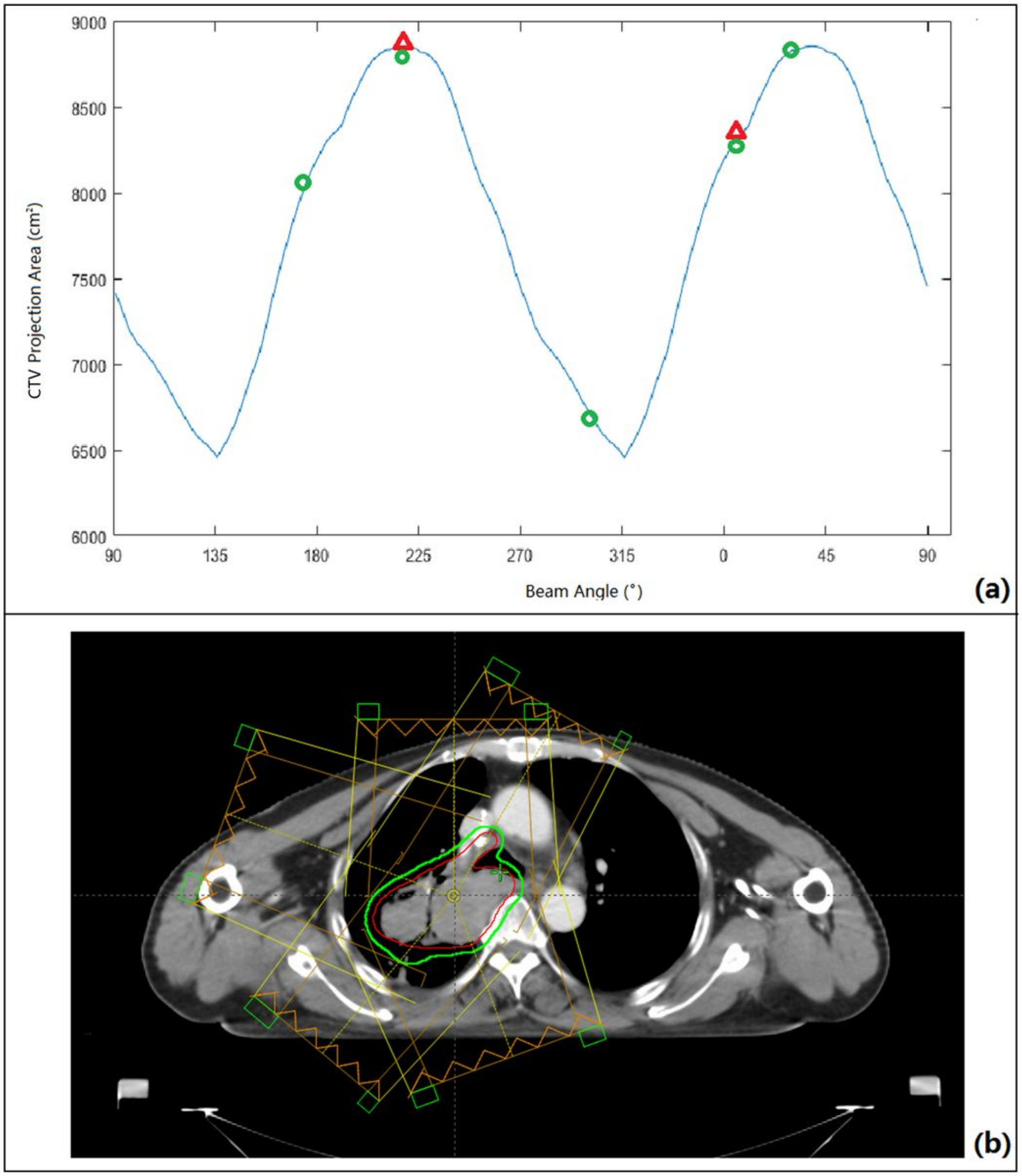

Figure 3

The example case's CTV projection area with respect to the beam angle is shown in panel (a). The selected beam angles (0°, 30°, 160°, 220°, and 290°) are indicated as green circles. The first and second maximum projection beam angles are indicated as red triangles; The axial slice view of the example case's beams are shown in panel (b).

Loading [MathJax]/jax/output/CommonHTML/fonts/TeX/fontdata.js

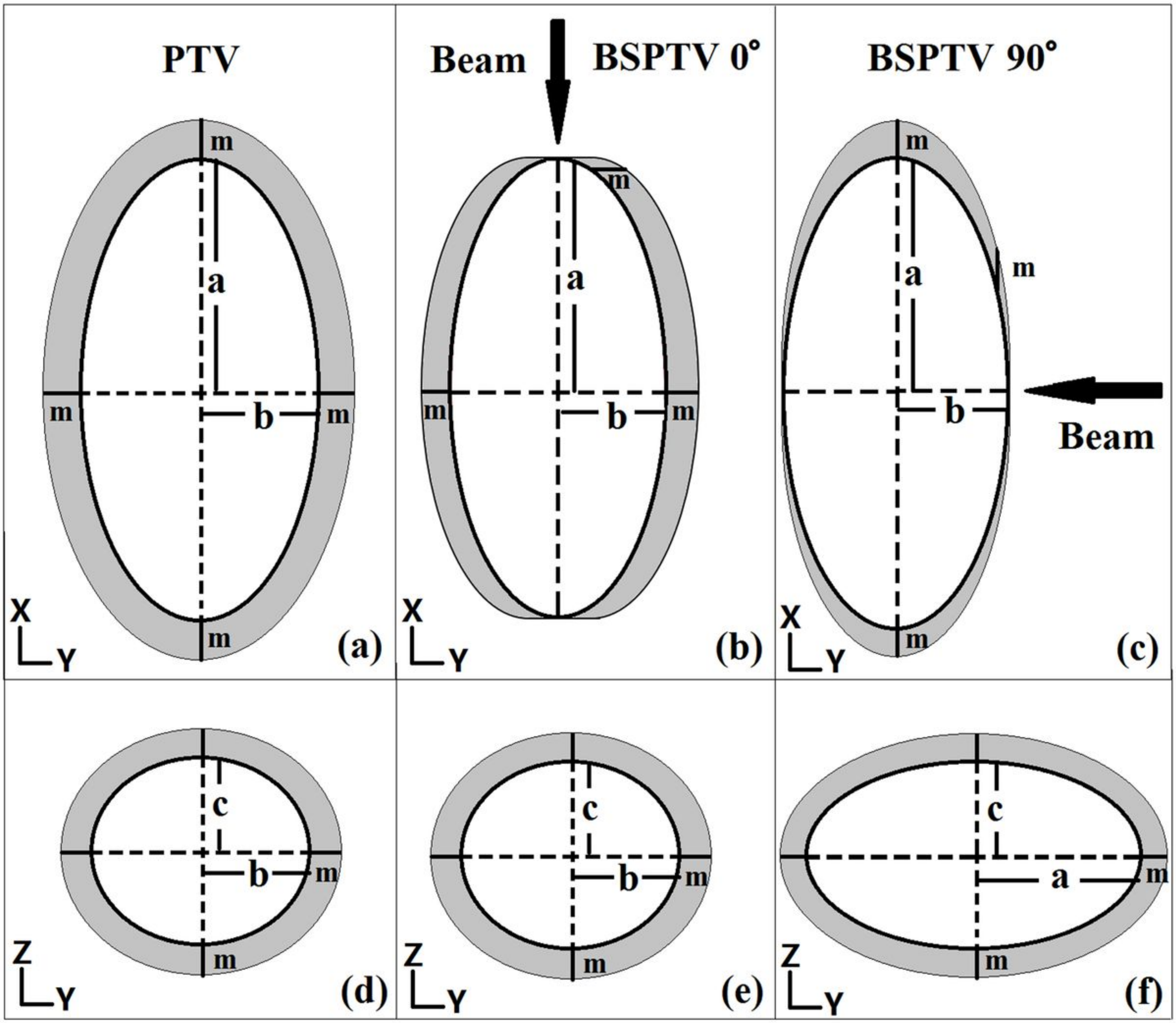

Figure 4

The projection area of the ellipsoid CTV and the conventional PTV in the XOY plane and YOZ plane are shown in panel (a) and (c). The CTV (thick black line) is margined isotropically with m (gray area) in three directions to PTV (thin black line). The projection areas of the ellipsoid CTV and BSPTV of beam 0⍰ in the XOY plane and YOZ plane are shown in panel (b) and (d). The margin area (gray area) of BSPTV of beam 0⍰ is smaller than that of the conventional PTV. The projection areas of the ellipsoid CTV and BSPTV of beam 90⍰ in the XOY plane and YOZ plane are shown in panel (c) and (e). The margin area (gray area) of BSPTV of beam 90⍰ is smaller than that of both the conventional PTV and BSPTV of beam 0⍰.

Loading [MathJax]/jax/output/CommonHTML/fonts/TeX/fontdata.js